Dielectric binary oxide films as waveguide laser media: a review

2008 J. Phys.: Condens. Matter 20 264011

(http://iopscience.iop.org/0953-8984/20/26/264011)

J. Phys.: Condens. Matter **20** (2008) 264011 (8pp) doi:10.1088/0953-8984/20/26/264011

Dielectric binary oxide films as waveguide laser media: a review

C Grivas and R W Eason

Optoelectronics Research Centre, University of Southampton, Southampton SO17 1BJ, UK

E-mail: chg@orc.soton.ac.uk

Received 2 November 2007, in final form 11 December 2007
Published 9 June 2008
Online at stacks.iop.org/JPhysCM/20/264011

Abstract

Sapphire (α-Al_2O_3), amorphous and polycrystalline Al_2O_3, tantalum pentoxide Ta_2O_5 and the sesquioxides Y_2O_3, Sc_2O_3, and Lu_2O_3 are excellent laser hosts due to their very good thermomechanical properties, broad transparency range and ease of doping with active ions. This article reviews recent research towards the realization of active optical films and the demonstration of gain and laser operation in the waveguides produced from these materials. Compound structures in which laser operation has been demonstrated are highlighted together with the applied fabrication techniques, and details of the laser performance are presented.

(Some figures in this article are in colour only in the electronic version)

1. Introduction

Waveguide lasers exhibit high optical confinement and excellent mode overlap of pump and laser beams, which results in high optical gain and low threshold. Another benefit derived from the planar waveguide configuration is the potential for device miniaturization and integration as other optical applications and components can be incorporated onto the same substrate that hosts the laser cavity. Binary metal oxide compounds such as sapphire (α-Al_2O_3), amorphous and polycrystalline aluminum oxide (Al_2O_3) the sesquioxides Y_2O_3, Sc_2O_3, and Lu_2O_3 and tantalum pentoxide (Ta_2O_5) are excellent laser hosts, due to their high transparency and its extensive range, which offers the prospect of low loss optical waveguides. Further attributes include their refractive index values, which allow for large index contrast, high mechanical strength, very good thermal conductivity and excellent compatibility with standard Si/SiO_2 technologies. In film form all these properties can be combined with the advantages of the waveguide designs and therefore make fabrication of optical waveguide films of these materials a useful aim for development of compact integrated sources and amplifiers.

There are in general two different approaches for the fabrication of waveguide structures. The first is to produce a step change in the refractive index by growing a film onto a substrate of lower refractive index. This route allows fabrication of relatively thick guides of high index contrast, and therefore, of high numerical aperture (NA). A large number of methods are routinely used to produce waveguide films including epitaxial processes (liquid phase epitaxy [1, 2], molecular beam epitaxy (MBE) [2] and pulsed laser deposition (PLD) [2, 3]), chemical vapor deposition (CVD) [4] and its variants such as low pressure, plasma and laser enhanced CVD, sputtering [5] and thermal bonding [6]. Further processing of the resultant layers with surface structuring techniques such as laser ablation [7], ion beam milling [8] reactive ion etching (RIE) [9], as well as ion beam implantation and wet chemical etching [10] can lead to the formation of rib- or ridge-type channel waveguides. Channel geometries offer the possibility to achieve lower pump thresholds than in planar formats as a result of the enhanced lateral confinement of the pump and laser modes in the formerly unguided plane.

In the second waveguide fabrication approach a waveguide region is defined inside an existing crystal by producing a refractive index change. Methods that are used for this purpose are ion diffusion [11], ion or proton implantation [12, 13], direct laser writing [14, 15] and ion or proton exchange [16, 17]. This second methodology lies outside the scope of this review however.

The remainder of this review is set out as follows. Section 2 focuses on the progress made in the growth of active transition metal and rare-earth (RE) doped sapphire and Al_2O_3 waveguide films and takes a closer look at the fabrication of those structures for which laser operation has been demonstrated. In sections 3 and 4 the development of RE doped layers of Ta_2O_5 and the sesquioxides Y_2O_3, Sc_2O_3, and Lu_2O_3 is reviewed, respectively, while fabrication details

of optically active Ta_2O_5 lasing structures are discussed. In section 5, results on the operation of waveguide lasers based on these materials are presented, while concluding remarks are made in section 6. We note that only reports on *functional* performance of the produced structures are discussed in terms of optical loss, photoluminescence (PL), gain, lasing, or amplification toward end waveguide applications.

2. Active waveguides based on sapphire and Al_2O_3 films

Optically active sapphire and Al_2O_3 films have been fabricated with the inclusions of various dopants, although the most intensively studied elements have been titanium (Ti) and erbium (Er). Ti:sapphire lasers are characterized by low peak emission cross section and short fluorescence lifetime and therefore high pump power densities are required to achieve efficient cw lasing. Guided wave designs for these sources can lead to considerably lower pump laser thresholds, provided that fabrication does not introduce any extra propagation loss. It is no surprise therefore, that a lot of attention has been directed towards the development of Ti:sapphire waveguides and a variety of techniques such as PLD [18–24], a combination of PLD with photolithography and Ar milling [8] or RIE [9], thermal diffusion of Ti_2O_3 into sapphire crystals [25], ion [26]/proton implantation [13] and femtosecond laser writing [27] have been utilized for their realization. Chromium (Cr) is another transition metal that has been studied as a dopant [28, 29] however, to a far lesser extent than Ti. Research on RE dopants, for the most part, concentrated on Er:Al_2O_3 for development of optical devices for the telecommunications wavelength window around 1550 nm [30–37]. Recently growth of Er:Al_2O_3 films with the inclusion of other RE co-dopant ions such as thulium (Tm^{3+}), and ytterbium (Yb^{3+}) has been reported with the aim of improving their PL response and broadening their emission to the range 1400–1700 nm [38–43].

2.1. Doping with transition metals

One of the most popular film fabrication techniques and so far the only one that has produced active films that exhibited laser action has been PLD. PLD allows for stoichiometric transfer of a target material on a substrate and high deposition rates, of the order of a few tens of microns per hour ($\sim$25 μm h^{-1} for Ti:sapphire films). The only requirement is matching of lattice constants and thermal expansion coefficients between active layer and substrate (or between active layers) to prevent formation of defects in the films, which in turn can act as sources of scattering loss. Its main drawback is the presence of micron size particulates in the ablated material, which are then transported towards the substrate and can be incorporated into the layer. This may lead to additional scattering losses and therefore limit the prospects for device development. However, careful optimization of growth parameters can reduce to a great extent this detrimental effect and recently laser operation of PLD grown active layers exhibiting losses below 0.1 dB cm^{-1} has been reported [44, 45].

The problem of particulates was evident from the very early attempts to fabricate Ti:sapphire [18, 19] films, as they exhibited poor optical quality and high propagation losses [20, 21]. Growth from molten Al–Ti alloy targets [22, 23] has proven effective in eliminating the presence of the particulates from the film surface, although no quantitative estimation of the impact of this approach on the loss level was reported. In the same report the growth temperature was identified as a means to control the valence state of the Ti ion dopants. With a view to developing laser devices it is of particular importance to maintain the Ti^{3+} state and minimize the presence of tetravalent titanium (Ti^{4+}) in the film as the latter could limit the laser performance by parasitic absorption. In another attempt to improve the optical quality of the films, a high speed rotating target [20] was used, an approach that led to a significant decrease in the density of the surface particulates. However, no quantitative information was provided about the magnitude of the reduction in propagation loss, which was initially as high as $\sim$8.7 dB cm^{-1}. To date, there are only two reports, both from our research group, on the realization of waveguide lasers (with planar [46] and rib [47] geometries) from Ti:sapphire layers and in the following we shall present details on their fabrication and characterization. The lasing films were grown to a thickness of $\sim$12 μm and on undoped sapphire substrates held at a temperature of $\sim$975 °C using a 100 W CO_2 laser as a heating source [24]. Depositions were carried out in an argon atmosphere, from single crystal Ti:sapphire targets with a doping level of 0.12 wt% Ti_2O_3. Ablation was provided by a KrF excimer laser (248 nm, pulse duration $\sim$20 ns) operated at 25 Hz and focused to an energy density of $\sim$4 J cm^{-2} on the Ti:sapphire target. Due to the anisotropic nature of sapphire, high quality single crystalline growth was a prerequisite for the use of the produced layers as laser media. Optimization of the process parameters and in particular of growth temperature, has led to the formation of films with a degree of crystal perfection and dopant levels comparable with the commercial bulk crystal used as target material for the deposition. Moreover, XRD analysis showed that the Ti^{3+} was incorporated substitutionally for the Al^{3+} in the correct lattice position. Spatially coherent, broadband PL emission with a full width half maximum (FWHM) of 130 nm and of several hundred microwatts of power was generated from the produced films when pumped with an Ar^+ laser with output powers up to 1 W thereby indicating their suitability as broadband light sources for interferometric applications [48].

The PLD grown Ti:sapphire films were further processed to fabricate rib waveguides in a two-step process involving photolithographic patterning and subsequent Ar^+ beam milling [8] and such a rib structure is shown in figure 1(a) The aim of this research was to develop a high repetition rate, short pulse waveguide laser for applications in optical coherence tomography (OCT), where large bandwidth, high brightness light sources are required. Channel waveguide geometries would add the possibility to obtain near-circular, single transverse mode laser beams, which would allow for integration of the channel waveguide lasers with the fiber optic interferometers used in OCT systems. Non-destructive loss measurements using the self-pumped phase conjugation

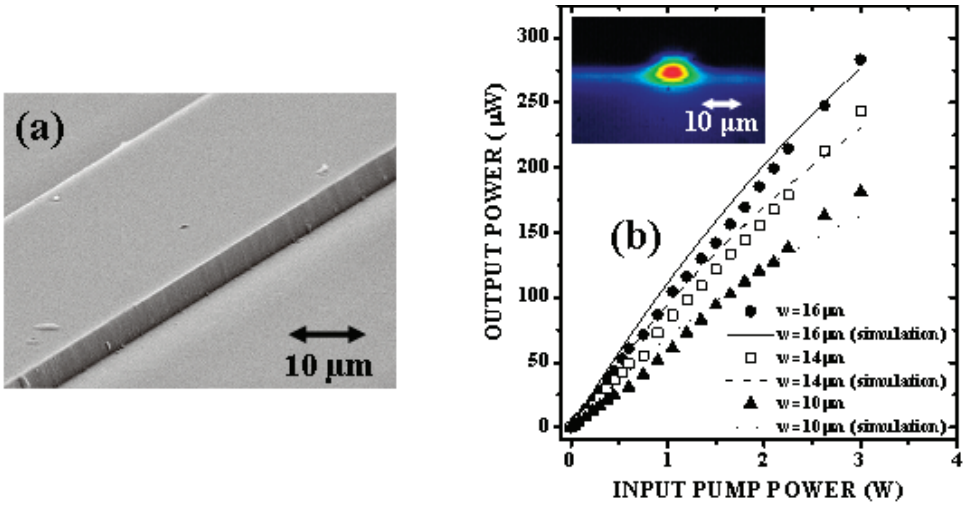

Figure 1. (a) SEM picture of a Ti:sapphire rib structure. (b) Fluorescence output as a function of Ar^+ laser pump power for rib waveguides with different cross sections. The points refer to experimental data, while the lines correspond to calculated fluorescence outputs.

technique (SPPC) [49] indicated that the process of structuring ribs on the surface of Ti:sapphire films by Ar^+ beam milling does not increase the level of propagation loss by more than ∼0.2 dB cm^{-1} compared to the background loss level of the PLD grown planar host. The fluorescence characteristics of the rib waveguides were studied using an Ar^+ pump laser, which was operated on all lines. Figure 1(b) shows the fluorescence output characteristics of channels with various cross sections together with the fluorescence profile of a channel with height and width of 5 and 10 μm, respectively, (inset). A number of these channels were optimized for single transverse mode propagation with measured beam propagation factors M_x^2 and M_y^2 equal to 1.12 and 1.16, for the in-plane and out-of-plane directions, respectively, to form arrays of fully diffraction limited, near-circular, single mode parallel emitting fluorescence sources from the same miniature sample. The latter has a potential for the integration of such devices in parallel OCT configurations and such a system with sixteen parallel Ti:sapphire ribs separated by a distance of 60 μm, generated a bandwidth of 174 nm and provided a depth resolution of 1.9 μm, which corresponds to 1.5 μm in the tissue [50].

There are only a very limited number of reports on the fabrication of Al_2O_3 films doped with other transition metals such as Cr having an end waveguide application as a goal. In one of these reports, amorphous Cr:Al_2O_3 layers were grown via MO-PECVD using the metal–organic precursor aluminum acetylacetonate (Al(acac)3) and chromium acetylacetonate (Cr(acac)3) as sources for Al and Cr, respectively [28]. After annealing with a CO_2 laser at ∼1200 °C the produced structures showed broadband fluorescence emission (700–1000 nm) and lifetimes of 1.60 ms were measured, with this latter value being close to the corresponding value for ruby bulk crystals. Epitaxial growth of Cr:sapphire films has been reported using simultaneous or sequential deposition of amorphous Al_2O_3 and metallic Cr on the same substrate via electron beam evaporation, followed by annealing at temperatures ranging from 800 to 1400 °C [29]. As result of this process substitutional incorporation of Cr for the Al ions in the correct lattice position was achieved.

2.2. Rare-earth doped Al_2O_3 waveguide films

PLD has also been extensively used for the growth of RE doped Al_2O_3 layers and the first of these reports was on the fabrication of Er:Al_2O_3 films by alternate PLD from Al_2O_3 and Er_2O_3 targets [31]. The as-deposited layers had a uniform dopant profile throughout their volume without any evidence of clustering and showed PL emission at 1.533 μm. Thermal annealing at 700 °C led to an increase of the PL peak intensity by a factor of 28 and of the lifetime from 0.2 μs to 4.4 ms. Further efforts focused on the enhancement of the PL emission by engineering the in-depth distribution [38] or both the in-depth distribution and in-plane concentration of Er^{3+} ions [39] in the films and led to longer PL lifetimes (>6 ms). Introduction of Yb^{3+} as a co-dopant in Er:Al_2O_3 films and optimization of their concentration ratio with respect to Er^{3+} ions as well as of their in-depth distribution, resulted in an increase in the PL intensity at 1.53 mm with respect to that recorded for layers doped only with Er^{3+} ions [40]. Recently co-doping of Er:Al_2O_3 layers with Tm [41, 42] as well as with Tm and Yb [43] by alternate PLD has been reported with the aim of extending the PL band of the Er:Al_2O_3 structure (1530–1600 nm) to the range from 1400 to 1700 nm. The fabricated structures exhibited indeed a broadband PL emission in the range 1400–1700 nm with a fairly flat profile and FWHM values of up 230 nm after annealing at 650 °C. It was also observed that the incorporation of Yb^{3+} as a co-dopant in the Er–Tm:Al_2O_3 films increases the lifetime without affecting the PL intensity and its FWHM value.

Other single step methods utilized for growth of Er:Al_2O_3 films were reactive co-sputtering [32] and atomic layer deposition (ALD), also known as atomic layer epitaxy [33]. In the former, layers were deposited on thermally oxidized Si wafers at a substrate temperature of 400 °C. They were amorphous, had smooth surface and exhibited a loss

of 0.25 dB cm^{-1} without any post-annealing, which is the lowest ever measured for as-deposited Er:Al_2O_3 films (to date, the corresponding loss values achieved for undoped Al_2O_3 were 0.11 and 0.2 dB cm^{-1} for planar and channel structures, respectively [51]). PL emission with a FWHM of ∼55 nm has been obtained and a relatively small up-conversion effect (2×10^{-24} m^3 s^{-1}) was observed for an Er concentration of 0.24 at.%. The most attractive features of the co-sputtering technique are the possibility to achieve homogeneous doping profiles and the relatively low deposition temperatures, which make the process compatible with microelectronic technologies. The Er:Al_2O_3 films grown by ALD, a method that allows controlled film growth on substrates with nanometer accuracy via a selected number of cycles of surface reactions of precursor gases, had a thickness of 2 μm and were further processed by photolithography and wet etching to produce ridge waveguides with height and width of 390 nm and 6 μm, respectively. The waveguides showed a broad emission spectrum with FWHM over 50 nm and strong Er-induced absorption, the maximum being 6.2 dB cm^{-1} for unpolarized light. The average Er concentration in the films was 2.3 wt% however, the uniformity of the doping profile required further improvement as suggested by the short fluorescence lifetimes (0.9 ms). Signal enhancement at 1.55 μm was observed in the films, which, however, saturated at ∼6 dB for a 3.9 cm long waveguide.

Net optical gain has been obtained from Er:Al_2O_3 spiral ridge waveguides realized by a multistep fabrication process [34]. The first step involved deposition of 600 nm thick Al_2O_3 layers on thermally oxidized Si(100) substrates by radio frequency magnetron sputtering followed by implantation with Er ions at energies ranging from 100 keV to 1.5 MeV. The latter resulted in a 0.28 at.% Er ion peak concentration with a flat profile in the area from 25 to 450 nm under the surface of the guide, which was a significant improvement from the Gaussian profile reported in earlier work [35]. The structure was annealed at 775 °C to remove any defects formed during the implantation process and spiral-formed ridge waveguides with height and width of 300 nm and 2 μm, respectively, were realized via photolithography and Ar atom beam etching. The last phase of the fabrication process involved growth of a 1.3 μm thick SiO_2 cladding layer on top of the ridge waveguide to reduce scattering losses and annealing of the completed structure at 700 °C for 30 min in N_2. The resultant 4 cm long structure exhibited loss as low as 0.35 dB cm^{-1} and provided a 2.3 dB net gain at 1.53 μm when pumped with 9 mW at 1.48 μm. The device was successfully integrated with wavelength division multiplexers to combine and separate pump and signal beams, thereby highlighting the potential of the whole approach for development of optical amplifiers and lasers in integrated optics. Potentials drawbacks of the ion implantation method are the requirement of post-annealing at high temperatures which may restrict the integration with other components produced in earlier fabrication steps as well as the difficulty to achieve optimal transverse doping concentration profiles.

Lastly, growth of Er:Al_2O_3 films has also been reported using CVD techniques such as PECVD [36, 37] and MO-PECVD [29]. PECVD of Er:Al_2O_3 films was carried out in a single step using trimethyl aluminum (TMA) and Er tri-chelate of 2,2,6,6-tetramethylheptane-3,5 dionate ($Er(thd)_3$) as Al and Er precursors, respectively [33]. The resultant layers showed broad room temperature PL at 1.533 μm with a FWHM of 55 nm, however they suffered from non-uniform distribution of Er^{3+} in their volume. In a second report by the same group a two-step process was adopted involving deposition of amorphous Al_2O_3 thin films by PECVD on Si(100) substrates at low temperature (200–300 °C) followed by implantation with Er^{3+} ions [33]. As Al precursor and oxidizing agent trimethylamine alane (TMAA) and nitrous oxide were used while argon served as the carrier gas for the TMAA. The process was characterized by low deposition rates of the order of 60 Å min^{-1} and the resultant structures exhibited a peak erbium concentration of 0.5 at.%. After thermal annealing at 850 and 950 °C in nitrogen, PL emission at 1.53 μm was observed even when the structures were pumped at wavelengths outside the Er^{3+} absorption bands. As such an effect was also observed in silicon-rich silica thin films where broadband excitation is due to the strong coupling between Er^{3+} and Si nanocrystals, it was speculated that the sensitizing species were most likely Al nanoclusters present at a very low concentration in the film. MO-PECVD Er:Al_2O_3 films were produced using (Al(acac)3) and $Er(thd)_3$ as precursors for Al and Er, respectively [34]. The films, which had an Er concentration of 0.446% were annealed at 800 °C to remove hydroxyl (OH) groups that could act as a source of loss and as quenching centers for the excited state energy. The measured propagation loss in the 3.5 cm long waveguides films was ∼5.7 dB cm^{-1} and an internal gain of 19 dB was obtained at 1.53 μm for a pump power of 45 mW at 1.48 μm (coupling efficiency ∼10%). A drawback of the CVD processes is the undesirable inclusions in the resultant films, which act as loss or quenching centers of the excited state energy, and can be removed by high temperature annealing.

3. Waveguides based on rare-earth doped tantalum pentoxide films

There is a continuous interest in the fabrication of high quality Ta_2O_5 films for microelectronic and microwave applications due to their high dielectric constant, good temperature and bias stability as well as the low values of defect density, dielectric loss, and leakage current [52] of this material. Furthermore, its large third order nonlinearity [53], high photosensitivity [54] and high optical damage threshold [55] make it suitable for a variety of optoelectronic applications. Optically active Ta_2O_5 films have been realized with the inclusion of RE ions such as Er^{3+} [56] praseodymium (Pr^{3+}) [57] and neodymium (Nd^{3+}) [58, 59] with the aim to develop compact sources and amplifiers for telecommunications applications.

Laser emission has recently been observed in Nd:Ta_2O_5 rib waveguides and their laser performance is discussed in the next section. Growth of the Nd:Ta_2O_5 films that hosted the ribs was performed on thermally oxidized silicon wafers by radio frequency (RF) magnetron sputtering from Ta_2O_5 targets with a doping level of 1 wt% and 0.5 wt% Nd_2O_3, respectively. The sputtering process was carried out in O_2/Ar

atmosphere at a background pressure of 30 mTorr and substrate temperature of 250 °C with a RF magnetron power density of 11 W cm^{-2} and Ar and O flow rates of 16 and 6 sccm, respectively. These optimized sputtering parameters yielded waveguides with low propagation loss (<0.2 dB cm^{-1}). Rib waveguides were then formed on the sputtered layers using photolithographic patterning and either Ar^+ beam milling [58] or reactive ion etching using a CHF_3–Ar etch process [59]. Ribs produced by the former method had a step depth of 1 μm (ribs 3 μm in height surrounded by planar waveguide areas with a thickness of 2 μm) and widths ranging from 2 to 20 μm. The widths of the reactive ion etched structures were from 1 to 20 μm and had a depth of 500 nm (ribs 2 μm in height surrounded by planar waveguide areas with a thickness of 1.5 μm). To reduce propagation loss due to oxygen defects the structures were annealed at temperatures of 480 °C in oxygen for 72 h.

Er:Ta_2O_5 layers have also been realized by Er^{3+} ion implantation (using energies from 190 to 380 keV) of undoped Ta_2O_5 films that had been grown via plasma-assisted deposition (ion plating) on silica substrates. Depending on the fabrication conditions, films exhibited propagation losses in the range from 2 to 10 dB cm^{-1} and showed PL at 1533 and 532 nm however, only after annealing at 400 °C [56]. In another report, Er:Ta_2O_5 and Pr:Ta_2O_5 films fabricated with the same method were embedded as central layers in optical microcavities consisting of a multidielectric thin film stack of alternating low (SiO_2) and high refractive index (Ta_2O_5) layers to investigate the radiation pattern of Er^{3+} and Pr^{3+} inside the cavity. It was demonstrated that their spontaneous emission can be spatially controlled, and these results were promising for development of devices in which the emitted light can be spatially confined in specific directions [56, 57].

4. Fabrication of active waveguides based on sesquioxide films

The sesquioxides Y_2O_3, Sc_2O_3, and Lu_2O_3 have the unique combination of properties required by laser hosts: high degree of mechanical strength and hardness, high thermal conductivity (up to 50% higher compared to YAG), ease of doping with RE ions and phonon energies as low as 600 cm^{-1}, which can lead to improved quantum efficiencies for laser devices. Although growth of undoped and RE doped Y_2O_3 waveguide films has been reported by many groups in recent years, with PLD being the prevailing fabrication method, Sc_2O_3, and Lu_2O_3 have received less attention. In the first of these reports, highly crystalline Er:Y_2O_3 layers were deposited on [0001]-oriented Al_2O_3 substrates via alternate PLD from yttrium metal and Er_2O_3 targets in an oxygen atmosphere [60]. They were textured along the [111] direction and showed very smooth surface features (average surface roughness of 2 nm for a 690 nm thick layer), which resulted in a relatively low propagation loss (<1 dB cm^{-1} at 800 nm). Studies that followed this work focused on PLD growth of Er:Y_2O_3 films with the inclusion of a second RE ion such as europium (Eu^{3+}) [61] and Yb^{3+} [62], as a means to reduce the probability of up-conversion phenomena that can cause quenching of the 1.55 μm Er emission. The Er:Eu:Y_2O_3 structures were grown on SiO_2/Si substrates from Er:Eu:Y_2O_3 targets in an oxygen atmosphere. They were stoichiometric, highly crystalline, and textured along the [111] direction and showed very smooth surface features, exhibiting low propagation loss (<1 dB cm^{-1} at 800 nm) [61]. Growth of Er:Yb:Y_2O_3 films was performed on c-cut Al_2O_3 substrates from ceramic Er:Yb:Y_2O_3 targets. The resulting structures were stoichiometric and showed PL emission at 1.53 μm. Lifetimes as high as 4.6 ms have been measured in films with an Er and total RE concentration of 3.5×10^{20} and 1.8×10^{21} at.% cm^{-3}, respectively, without any evidence of significant up-conversion [62]. Finally PLD formation of Tm^{3+} doped Y_2O_3 films has also been studied [63]. The resultant layers were highly crystalline, with stoichiometry and fluorescence lifetimes similar to those of bulk crystals with the same doping level.

Besides PLD, formation of Er:Y_2O_3 layers has been reported by radical enhanced ALD using $Y(thd)_3$ and $Er(thd)_3$ as Y_2O_3 and Er_2O_3 precursors and O radicals as the oxidizing agent. The process involved deposition of Y_2O_3 and Er_2O_3 in an alternate fashion at a relatively low temperature (350 °C) [64]. Films were typically 320 Å thick with Er^{3+} concentration of 9 at.%, and exhibited PL at room temperature without any post-deposition annealing. The effective absorption cross section for Er^{3+} in the films was estimated to be of the order of 10^{-18} cm^2, which corresponds to an improvement of three orders of magnitude with respect to the corresponding value reported for Er^{3+} ions in a SiO_2 host, suggesting the potential to achieve functional devices requiring pump powers. In another report, a signal enhancement of 10 dB at 1.535 μm for launched pump powers as low as 1 mW at 1480 nm has been obtained from Er:Y_2O_3 ridge waveguides. The latter had a height of 80 nm and widths varying from 4 to 10 μm and were fabricated by photolithography and Ar^+ beam milling in films that had been grown by reactive co-sputtering from metallic yttrium and erbium targets [65]. The same research group has also reported growth of Er:Y_2O_3 optical waveguides via spray pyrolysis using $Y(thd)_3$ and erbium acetylacetonate (Er(acac)3) as sources for Al and Cr, respectively. The as-deposited films exhibited room temperature luminescence that was sharply peaked at 1.54 μm however, they suffered from the presence of hydroxyl groups, which possibly contributed to the attenuation at 1.54 μm [66].

Sc_2O_3 has also been studied as a film matrix for RE ions and growth of highly crystalline Nd:Sc_2O_3 layers on (0001)-oriented (α-Al_2O_3) substrates by PLD has been reported [67]. Films had a thickness of 3 μm and were highly textured in the [111] direction. Their emission and excitation spectra were very similar to those of the bulk crystal target with no evidence of spectral line broadening. However, they exhibited high propagation loss (~37 dB cm^{-1}), which severely restricted their applicability for device development. Recently PLD layer-by-layer growth of Er:Sc_2O_3 thin films has been studied [68] to identify possible irregularities in the growth of the first few atomic layers, which due to their position close to the film–substrate interface could act as sources of loss in the waveguide. Growth was performed on [100]- and [111]-oriented Sc_2O_3 as well as on [100]-oriented

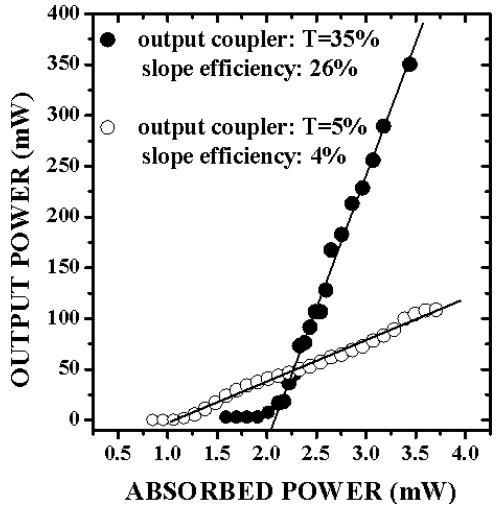

Figure 2. Output power from a 12.3 μm thick Ti:Al_2O_3 planar waveguide as a function of absorbed pump power for two output couplers with transmission of 35% and 5%, at the lasing wavelength.

Y_2O_3 substrates, and films were highly crystalline and highly textured in an orientation defined by the substrate. Finally, there are only a limited number of reports on Lu_2O_3 active films, (all on Eu:Lu_2O_3 layers [69–71]) however, not for end waveguide applications but for phosphors or scintillators.

5. Waveguide lasers based on binary oxide films

Although there are a significant number of reports on the fabrication of waveguide films of binary oxides for development of lasers, to our knowledge successful laser operation has so far been reported only for Ti:Al_2O_3 and Nd:Ta_2O_5 structures. The fabrication of the devices has been detailed in sections 2.1 and 3 respectively, and in the following their laser performance will be discussed.

5.1. Ti:sapphire waveguide laser

Successful laser operation has been demonstrated in Ti:Al_2O_3 waveguide films grown by PLD as detailed in section 2.1. The laser cavity was formed by attaching to the end faces of the sample two thin dielectric mirrors with high reflectivity (99.4%) and transmission of 86% at the lasing and pump wavelength, respectively. Laser operation was achieved at room temperature with an Ar^+ pump laser operating on all lines at an absorbed pump power threshold of 0.72 W [46]. The laser emission was centered near 808 nm and had a π polarization regardless of the polarization state of the pump beam due to the larger emission cross section of the waveguides for the π compared to the σ polarization component. A maximum output of 357 mW for 3.44 W of absorbed power and a slope efficiency of 26% were obtained using an output coupler with a transmission of 35%. The output characteristics as a function of absorbed pump power are shown in figure 2, for two different values of output coupler transmission. A loss of 1.5 dB cm^{-1} deduced for the film by the Findlay–Clay method [72], was assumed to originate from surface scattering caused by particulates present on the film.

Laser operation has also been demonstrated in Ti:Al_2O_3 rib waveguides structured on the surface of these films by photolithography and Ar^+ beam milling [8]. Experiments were performed at room temperature with an Ar^+ pump laser operating on all lines using an extended laser cavity configuration, which allowed for introduction of intra-cavity optical elements for modulation or tuning [47]. CW laser emission was obtained in ribs with height and width of 3.5 and 10 μm, respectively, at an absorbed pump power threshold of 265 mW, which was more than a factor of 2 lower than the one obtained from their planar counterpart. It was centered at 792.5 nm and π polarized regardless of the polarization state of the pump beam. The laser spectral output at an absorbed pump power of 350 mW together with the laser mode profile (inset) is shown in figure 3(a). Measurement of the beam propagation factors M^2 showed near-diffraction limited laser emission from the ribs with values of $M_x^2 = 1.3$ and

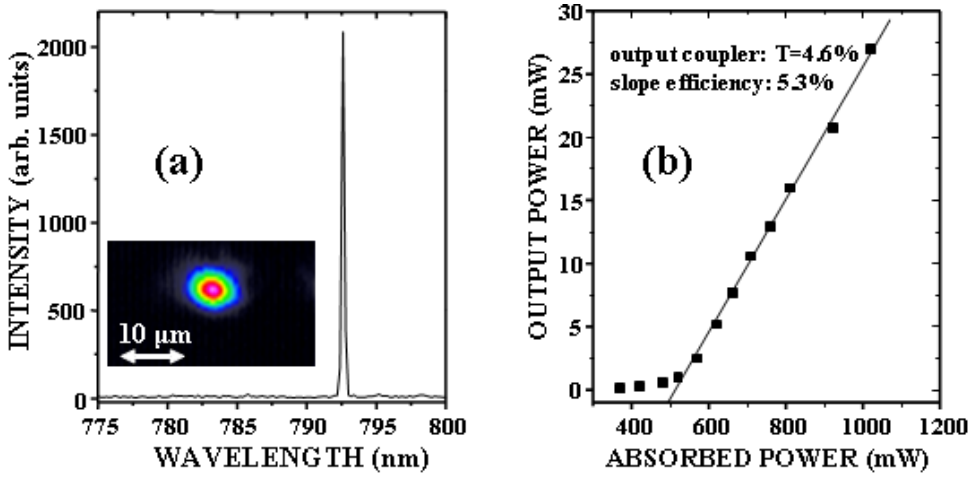

Figure 3. (a) Laser spectral output from rib waveguide with width and height of 10 and 3.5 μm respectively, for an absorbed pump power of 350 mW. A laser mode profile originating from this structure is shown in the inset. (b) Laser characteristics of the same rib waveguide for an output coupler with transmission 4.6%.

$M_y^2 = 1.2$ for the horizontal and perpendicular directions, respectively. By replacing the HR output mirror by an output coupler with a 4.6% transmission at the lasing wavelength the threshold increased from 265 to 315 mW. The input/output laser characteristics obtained with the 4.6% output coupler are shown in figure 3(b). The rib waveguide laser emitted 27 mW for 1 W of absorbed pump power, and a slope efficiency of 5.3% was obtained. To date, Ti:sapphire waveguide lasers with a channel geometry have also been realized by proton implantation [73] and Ti_2O_3 in-diffusion [74], methods that do not involve fabrication of a waveguide film.

5.2. Neodymium doped tantalum pentoxide waveguide laser

Laser operation of the Nd:Ta_2O_5 rib waveguides was demonstrated with a Ti:sapphire pump laser [58]. The laser resonator was formed by attaching a high reflectivity (HR) mirror to the input face and a set of successive output couplers with reflectivities ranging from 40% to 99.9% to the output face of the waveguide. For ribs fabricated by Ar^+ beam milling, a cavity formed by two HR mirrors has led to laser emission at an absorbed pump power threshold of 87 mW. When the HR output mirror was substituted with a 9% output coupler the threshold value increased to 120 mW and a slope efficiency of 1.0% was obtained. The laser output was TE polarized regardless of the polarization state of the pump beam. A propagation loss of $\sim$2 dB cm^{-1} at the lasing wavelength was derived using the Findlay–Clay method [72], which was higher than the loss exhibited by unstructured Nd:Ta_2O_5 planar waveguides ($\sim$0.7 dB cm^{-1}), thus indicating that the rib fabrication process has increased the background attenuation. The laser spectrum showed that lasing occurred at many wavelengths in the range between 1060 and 1080 nm, most likely as a result of the broad fluorescence bandwidth of Nd in amorphous hosts, and the use of resonator mirrors with broadband reflectivity.

Laser operation was also observed in ribs patterned by reactive ion etching. Laser emission was obtain in ribs with a width of 18 μm and a step depth of 500 nm (total height 2 μm), at an absorbed pump power threshold of 2.7 mW when a cavity with two HR mirrors was used [59]. The thresholds for the 8.4%, 17.8%, and 34.7% output couplers were 6.1, 12.9, and 33.8 mW respectively, and a slope efficiency of 21% was obtained with 34.7% output coupling. Lasing was observed at many wavelengths in the range between 1060 and 1070 nm, but also at 1.375 μm, when an HR/HR cavity was used, however, at a higher threshold (298 mW). The propagation loss as derived by a Findlay–Clay analysis was 0.2 dB cm^{-1} at the lasing wavelength. The propagation loss and laser threshold values were lower compared to those obtained from the Ar^+ beam etched ribs as a result of the improved surface quality of the ribs. Lifetime measurements of the excited state showed a dependence on the pump power, thus indicating the existence of Auger up-conversion. Up-conversion effects in the Nd:Ta_2O_5 rib waveguides and their influence on the laser performance was the subject of a later study [75, 76], where it was suggested that an energy transfer up-conversion (ETU) process between closely positioned Nd^{3+} ions was responsible for the reduced lifetime of the upper laser level. The induced increase of the pump power threshold was theoretically predicted to be proportional to the ETU rate, which was confirmed by the threshold observed experimentally for different output coupling mirrors.

6. Conclusions

There has been a large effort over the last few years to combine the attributes of waveguide geometries with the favorable optical and material properties of crystalline binary oxides such as Al_2O_3, Ta_2O_5 and the sesquioxides Y_2O_3, Sc_2O_3, and Lu_2O_3 for the development of active waveguide devices and in particular of laser sources. In this review we have seen an extensive range of waveguide fabrication techniques utilized for this purpose and highlighted the approaches that led to a successful demonstration of waveguide laser operation. Although for some of these materials progress has reached the level of device prototype development, substantial improvement of the optical and structural properties of the produced structures is still required to obtain fully functional devices for integrated optics applications.

References

[1] Ferrand B, Chambaz B and Couchaud M 1999 *Opt. Mater.* **11** 101
[2] Burkhalter R, Dohnke I and Hulliger J 2001 *Prog. Cryst. Growth Charact. Mater.* **42** 1
[3] Jelínek M, Lančok J, Šonský J, Oswald J, Šimečková M, Jastrabík L, Studnička V, Grivas C and Hříbek P 1998 *Czech. J. Phys.* **48** 577
[4] Studebaker D B, Stauf G T, Baum T H, Marks T J, Zhou H and Wong G K 1997 *Appl. Phys. Lett.* **70** 565
[5] Kubodera K, Nakano J, Otsuka K and Miyazawa S 1978 *J. Appl. Phys.* **49** 65
[6] Brown C T A, Bonner C L, Warburton T J, Shepherd D P, Tropper A C, Hanna D C and Meissner H E 1997 *Appl. Phys. Lett.* **71** 1139
[7] Lančok J, Jelínek M, Bulíř J and Macháč P 1998 *Laser Phys.* **8** 303
[8] Grivas C, Shepherd D P, May-Smith T C, Eason R W, Pollnau M, Crunteanu A and Jelínek M 2003 *IEEE J. Quantum Electron.* **39** 501
[9] Crunteanu A, Pollnau M, Jänchen G, Hibert C, Hoffmann P, Salathé R P, Eason R W, Grivas C and Shepherd D P 2002 *Appl. Phys.* B **75** 15
[10] Crunteanu A, Jänchen G, Hoffmann P, Pollnau M, Buchal C, Petraru A, Eason R W and Shepherd D P 2003 *Appl. Phys.* A **76** 1109
[11] Schmidt R V and Kaminow I P 1974 *Appl. Phys. Lett.* **25** 458
[12] Chandler P J, Zhang L and Townsend P D 1991 *Nucl. Instrum. Methods Phys. Res.* B **59** 1223
[13] Laversenne L, Hoffmann P, Pollnau M, Moretti P and Mugnier J 2004 *Appl. Phys. Lett.* **85** 5167
[14] Miura K, Qiu J R, Inouye H, Mitsuyu T and Hirao K 1997 *Appl. Phys. Lett.* **71** 3329
[15] Svalgaard M, Poulsen C V, Bjarklev A and Poulsen O 1994 *Electron. Lett.* **30** 1401
[16] Ramaswamy R V and Srivastava R 1988 *J. Lightwave Technol.* **6** 984
[17] Jackel J L, Rice C E and Veselka J J 1982 *Appl. Phys. Lett.* **41** 607
[18] Dyer P E, Jackson S R, Key P H, Metheringham W J and Schmidt M J J 1996 *Appl. Surf. Sci.* **96–98** 849

[19] Dyer P E, Gonzalo J, Key P H, Sands D and Schmidt M J J 1997 *Appl. Surf. Sci.* **110** 345
[20] Jelínek M, Eason R W, Lančok J, Anderson A A, Grivas C, Fotakis C, Jastrabik L, Flory F and Rigneault H 1998 *Thin Solid Films* **322** 259
[21] Uetsuhara H, Goto S, Nakata Y, Vasa N, Okada T and Maeda M 1999 *Appl. Phys.* A **69** S719
[22] Willmott P R, Manoravi P, Huber J R, Greber T, Murray T A and Holliday K 1999 *Opt. Lett.* **24** 1581
[23] Manoravi P, Willmott P R, Huber J R and Greber T 1999 *Appl. Phys.* A **69** S865
[24] Anderson A A, Eason R W, Jelínek M, Grivas C, Lane D, Rodgers K, Hickey L M B and Fotakis C 1997 *Thin Solid Films* **300** 68
[25] Hickey L M B, Martins E, Roman J E, Brocklesby W S and Wilkinson J S 1996 *Opt. Lett.* **21** 597
[26] Morpeth L D and McCallum J C 2000 *Appl. Phys. Lett.* **76** 424
[27] Apostolopoulos V, Laversenne L, Colomb T, Depeursinge C, Salathé R P, Pollnau M, Osellame R, Cerullo G and Laporta P 2004 *Appl. Phys. Lett.* **85** 1122
[28] Yu N, Wen Q, Clarke D R, McIntyre P C, Kung H, Nastasi M, Simpson T W, Mitchell I V and Li D Q 1995 *J. Appl. Phys.* **78** 5412
[29] Mahnke M, Wiechmann S, Heider H J, Blume O and Müller J C 2001 *Int. J. Electron. Commun. (AEU)* **55** 342
[30] Polman A 1997 *J. Appl. Phys.* **82** 1
[31] Serna R and Afonso C N 1996 *Appl. Phys. Lett.* **69** 1541
[32] Musa S, van Weerden H J, Yau T H and Lambeck P V 2000 *IEEE J. Quantum Electron.* **36** 1089
[33] Solehmainen K, Kapulainen M, Heimala P and Polamo K 2004 *IEEE Photon. Technol. Lett.* **16** 194
[34] van den Hoven G N, Koper R J I M, Polman A, van Dam C, van Uffelen J W M and Smit M K 1996 *Appl. Phys. Lett.* **68** 1886
[35] van den Hoven G N, Snoeks E, Polman A, van Uffelen J W M, Oei Y S and Smit M K 1993 *Appl. Phys. Lett.* **62** 3065
[36] Chryssou C E and Pitt C W 1998 *IEEE J. Quantum Electron.* **34** 282
[37] Chryssou C E, Kenyon A J, Smeeton T M, Humphreys C J and Hole D E 2004 *Appl. Phys. Lett.* **85** 5200
[38] Serna R, Jimenez de Castro M, Chaos J A, Afonso C N and Vickridge I 1999 *J. Lumin.* **75** 4073
[39] Serna R, Jimenez de Castro M, Chaos J A, Suarez-Garcia A, Afonso C N, Fernández M and Vickridge I 2001 *J. Appl. Phys.* **90** 32
[40] Suarez-Garcia A, Serna R, Jimenez de Castro M, Afonso C N and Vickridge I 2004 *Appl. Phys. Lett.* **84** 2151
[41] Xiao Z, Serna R, Afonso C N and Vickridge I 2005 *Appl. Phys. Lett.* **87** 111103
[42] Xiao Z, Serna R, Afonso C N and Vickridge I 2007 *J. Appl. Phys.* **101** 033112
[43] Xiao Z, Serna R, Afonso C N, Chen G and Vickridge I 2007 *J. Lumin.* **122/123** 32
[44] Grivas C, May-Smith T C, Shepherd D P and Eason R W 2004 *Opt. Commun.* **229** 355
[45] May-Smith T C, Grivas C, Shepherd D P, Eason R W and Healy M J F 2004 *Appl. Surf. Sci.* **223** 361
[46] Anderson A A, Eason R W, Hickey L M B, Jelinek M, Grivas C, Gill D S and Vainos N A 1997 *Opt. Lett.* **22** 1556
[47] Grivas C, Shepherd D P, May-Smith T C, Eason R W and Pollnau M 2005 *Opt. Express* **13** 210
[48] Pollnau M, Salathé R P, Bhutta T, Shepherd D P and Eason R W 2001 *Opt. Lett.* **26** 283
[49] Brülisauer S, Fluck D, Solcia C, Pliska T and Günter P 1995 *Opt. Lett.* **20** 1773
[50] Bourquin S, Laversenne L, Rivier S, Lasser T, Salathé R P, Pollnau M, Grivas C, Shepherd D P and Eason R W 2005 *Proc. SPIE* **5690** 209
[51] Bradley J D B, Ay F, Wörhoff K and Pollnau 2007 *Appl. Phys.* B **89** 311
[52] Chaneliere C, Autran J L, Devine R A B and Balland B 1998 *Mater. Sci. Eng.* **22** 269
[53] Tai C Y, Grivas C and Wilkinson J S 2004 *IEEE Photon. Technol. Lett.* **16** 1522
[54] Tai C Y, Wilkinson J S, Perney N M B, Netti M C, Cattaneo F, Finlayson C E and Baumberg J J 2004 *Opt. Express* **21** 5110
[55] Jasapara J, Nampoothiri A V V and Rudolph W 2001 *Phys. Rev.* B **63** 045117
[56] Rigneault H, Flory F, Monneret S, Robert S and Roux L 1996 *Appl. Opt.* **35** 5005
[57] Robert S, Rigneault H and Lamarque F 1998 *J. Opt. Soc. Am.* B **15** 1773
[58] Unal B, Tai C Y, Shepherd D P, Wilkinson J S, Perney N M B, Netti M C and Parker G J 2005 *Appl. Phys. Lett.* **86** 021110
[59] Unal B, Netti M C, Hassan M A, Ayliffe P J, Charlton M D B, Lahoz F, Perney N M B, Shepherd D P, Tai C Y, Wilkinson J S and Parker G J 2005 *IEEE J. Quantum Electron.* **41** 1465
[60] Korzenski M B, Lecoeur P, Mercey B, Carny P and Doualan J L 2001 *Appl. Phys. Lett.* **78** 1210
[61] Pons-Y-Moll O, Perriere J, Million E, Defourneau R M, Defourneau D, Vincent B, Essahiaoui A, Boudrioua A and Seiler W 2002 *J. Appl. Phys.* **92** 4885
[62] Dikovska A O G, Atanasov P A, Jiménez de Castro M, Perea A, Gonzalo J, Afonso C N and Garcia López J 2006 *Thin Solid Films* **500** 336
[63] Huignard A, Aron A, Aschehoug P, Viana B, Théry J, Laurent A and Perrière J 2000 *J. Mater. Chem.* **10** 549
[64] Van T T and Chang J P 2005 *Appl. Phys. Lett.* **87** 011907
[65] Hoekstra T H, Lambeck P V, Albers H and Popma T J A 1993 *Electron. Lett.* **29** 581
[66] Hoekstra T H, Hilderink L T H, Lambeck P V and Popma T J A 1992 *Opt Lett.* **17** 1506
[67] Kuzminykh Y, Kahn A and Huber G 2006 *Opt. Mater.* **28** 883
[68] Gün T, Kuzminykh Y, Petermann K, Scheife H and Huber G 2005 *Appl. Phys.* A **80** 209
[69] Bär S, Huber G, Gonzalo J, Perea A and Paszti F 2005 *Mater. Sci. Eng.* B **105** 30
[70] Martinet C, Pillonnet A, Lančok J and Garapon C 2007 *J. Lumin.* **126** 807
[71] Guo H, Yin M, Dong N, Xu M, Lou L and Zhang W 2005 *Appl. Surf. Sci.* **243** 245
[72] Findlay D and Clay R A 1966 *Phys. Lett.* **20** 277
[73] Grivas C, Shepherd D P, Eason R W, Laversenne L, Moretti P, Borca C N and Pollnau M 2006 *Opt. Lett.* **31** 3450
[74] Hickey L M B, Apostolopoulos V, Eason R W, Wilkinson J S and Anderson A A 2004 *Opt. Soc. Am.* B **21** 1452
[75] Lahoz F, Martin I R, Shepherd D P, Wilkinson J S and Hassan M A 2006 *Chem. Phys. Lett.* **421** 198
[76] Lahoz F and Hassan M A 2006 *Chem. Phys. Lett.* **426** 135